Asymmetry determines the effects of natural ceramides on model membranes†‡

Dolores C. Carrer, Eva Kummer, Grzegorz Chwastek, Salvatore Chiantia and Petra Schwille*

Received 28th January 2009, Accepted 26th March 2009
First published as an Advance Article on the web 1st May 2009
DOI: 10.1039/b901883b

Ceramides can dramatically influence the lateral organization of biological membranes. In particular, ceramide-induced alterations of protein-lipid domains can be involved in several cellular processes, ranging from senescence to immune response. In this context, an important role is played by the length of the fatty acid bound to the sphingosine moiety. Asymmetric, heterogeneous ceramides, with more than 20 or less than 16 carbon atoms in the fatty acyl chain, in fact exert diverging effects *in vivo* if compared to their symmetric counterparts. In this work, we investigated the role of ceramide asymmetry and heterogeneity in model membranes showing raft-like phase separation, using a combination of fluorescence imaging, atomic force microscopy, fluorescence correlation spectroscopy and differential scanning calorimetry. We show that ceramide produced enzymatically from natural mixtures of sphingomyelin can dramatically alter the mixing behaviour of proteins and lipids in the membrane, inducing a homogenization of the bilayer. Furthermore, we characterized the physical properties of coexisting lipid phases at equilibrium in membranes with varying ceramide content, emphasizing the differences between symmetric-homogeneous and asymmetric-heterogeneous ceramides. While symmetric ceramides always produce enhanced order, asymmetric ceramides display a more complex behavior similar to that of cholesterol. Our results might help contribute to a more precise understanding of the rearrangements induced by different kinds of ceramide generation in cellular membranes.

Introduction

Ceramide is a bio-active sphingolipid involved in various cell signaling pathways, acting as a second messenger in processes such as apoptosis, senescence, immune response, bacterial and viral pathogenesis, and cell cycle arrest.[1–5] In response to specific stimuli, ceramide concentration in the physiological context can reach 10–20% of the total lipid content,[6,7] although the local concentration in a particular membrane compartment may be higher.

Biophysical studies of model membranes containing ceramides have shown that they give rise to ceramide rich phases/domains,[8–10] promote the formation of nonlamellar structures[11] and induce transbilayer flip–flop[12] and the budding of small vesicles from giant unilamellar vesicles.[13,14] The literature on the biophysical properties of ceramides has become extensive in the last few years, and for reviews the reader is directed to the excellent works by Morales and collaborators[15] and Goñi and Alonso.[16] We will only discuss here work relevant for the understanding of the effects of fatty acid chain composition of ceramides.

The chain composition profile of ceramide molecules has been shown to be linked to dramatically different effects in cancer cells, with symmetric, homogeneous ceramides inducing apoptosis and asymmetric, heterogeneous ceramides supporting higher proliferation and chemoresistence (see ref. 17 and references therein). While symmetric ceramides can only exhibit a homogenous population of molecules with fatty acid chain lengths similar to that of the sphingosine moiety (C16 or C18), asymmetric ceramides are also heterogenous, since they can have fatty acid chain lengths either much shorter or much longer than the sphingosine moiety, and can also exhibit a double bond, as in the case of C24:1, relatively abundant in natural ceramides. This difference between the membrane effects of symmetric and asymmetric ceramides has also been observed in membrane model systems. In mixtures with DMPC, C16 ceramide shows different mixing behaviour and different domain morphologies when compared to C24:1 ceramide.[18] Symmetric ceramides have been shown to induce the formation of gel phases with high phase transition temperatures, to increase membrane order and to decrease the diffusion coefficient in the membrane.[19,9,20–22] Conversely, long asymmetric ceramides have been shown to be able to interdigitate the fatty acid chain into the opposing hemilayer,[23] while short asymmetric ceramides are able to induce partially interdigitated conformations.[24] Long asymmetric ceramides induce the formation of high temperature melting phases and produce condensation and increased order in mixtures with phospholipids below the phase transition pressure.[8] Short asymmetric ceramides induce the formation of phases with phase transition temperatures lower that symmetric ceramides[25] and produce an increase in the diffusion coefficient of the lipids in the ordered phase when compared with symmetric

Biotechnology Centre, Technical University of Dresden, Tatzberg 47–51, 01307 Dresden, Germany. E-mail: petra.schwille@biotec.tu-dresden.de
† This paper is part of a *Soft Matter* themed issue on Membrane Biophysics. Guest editor: Thomas Heimburg.
‡ Electronic supplementary information (ESI) available: Examples of the heterogeneity of GUVs prepared with the mixture composed of DOPC:BSM:BCer:Chol 2:1:1:1. See DOI: 10.1039/b901883b

ceramides.[26] Thus symmetric, homogeneous ceramides display a behaviour that is in many ways opposite to that shown by asymmetric, heterogeneous ceramides. While symmetric ceramides always increase order, asymmetric ceramides seem to have a more complex behavior, inducing order in some cases while increasing disorder in other cases. We have hypothesized in previous work that the transition entropy changes of saturated phospholipid-asymmetric ceramide mixtures could be explained by a simultaneous induction by asymmetric ceramides of disorder in gel phases and order in fluid phases, thus producing an effect similar to that of cholesterol.[24]

In this work we aim to further understand the difference in the effects of long chain asymmetric, heterogeneous ceramides *versus* long chain symmetric, homogeneous ceramides on model membranes, this time in mixtures with unsaturated phospholipids and cholesterol. We have chosen a raft mixture of dioleoylphosphatidylcholine/brain sphingomyelin/cholesterol (DOPC/BSM/Chol) and replaced BSM by brain ceramides (BCer) either by the activity of sphingomyelinase (SMase) or by pre-mixing the lipids. We compare the resulting membranes with similar membranes containing C18Ceramide (C18Cer).

We find a clear difference between the effects of C18Cer and brain ceramide. While C18Cer can only induce higher order and stronger compartmentalization in the membrane, brain ceramides have a dual effect depending on concentration: they produce the homogeneization of the membrane at physiological concentrations, making ordered phases more fluid and disordered phases more rigid, while inducing order and compartmentalization at higher concentrations.

Results and discussion

Sphingomyelinase activity on a domain exhibiting bilayer produces a reshuffling of the lipids and a subsequent new domain separation

Sphingomyelinase was applied to a supported lipid bilayer composed of DOPC:BSM:Chol 2:2:1. This mixture exhibits liquid ordered–liquid disordered phase coexistence at room temperature (Fig. 1a). Brain sphingomyelin contains 34 mole% of asymmetric molecules, with very long fatty acids (C22–24). Of this 34 mole%, 59% are also unsaturated (containing a 24:1 fatty acid chain). Fifty percent of the molecules are symmetric, with long fatty acids (C16–18). Upon SMase mediated conversion of BSM to Cer, a change can be observed in each of the images moving from the top left to the bottom right. Normally the whole bilayer would show these changes at the same time. In this case the changes can be traced as a wave front through the image due to an inhomogeneous distribution of the enzyme in the sample. The first change observed is that contrast is lost between the domains, probably due to a higher partitioning of the fluorescent probe into the ordered domains (Fig. 1, insert, region 1). At a certain time point, the membrane looks homogeneous, without distinguishable domains (Fig. 1b, c and d, region 2 in insert). Subsequently, small dark domains re-appear and grow in size with time (Fig. 1, insert, region 3). In some parts of the image, large (5–8 μm) areas of the brighter phase appear surrounded by an annulus of these new dark domains. At long incubation times the bilayer becomes detached from the mica in some regions, the lipid is lost into the bulk aqueous phase and the mica surface is exposed (Fig. 1f, *).

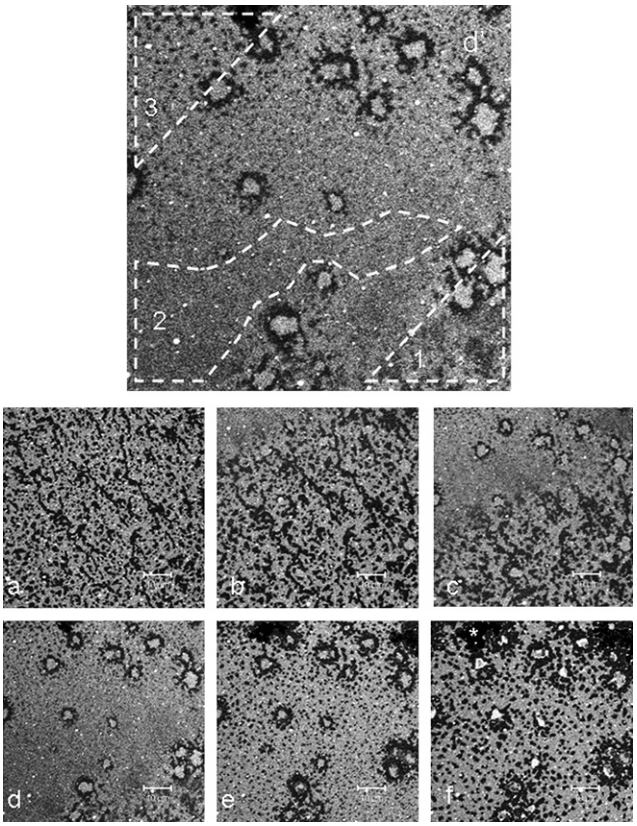

Fig. 1 Supported lipid bilayer under the activity of sphingomyelinase imaged by confocal microscopy. The initial lipid composition is DOPC:BSM:Chol 2:2:1. Pictures are taken at times (a) 0 min, (b) 15 min, (c) 18 min, (d) 21 min, (e) 30 min, (f) 63 min. The picture labeled d' is a zoom-in of image d. The regions marked indicate places where (1) the domains show decreased contrast (2) no domains can be distinguished (3) small dark domains re-appear. The concentration of enzyme was 37.5 mU/ml. The bar indicates 10 μm. The fluorescent probe used is BODIPYChol. The asterisk indicates a region where the bilayer has been lost.

Reshuffling of lipids produces concomitant reshuffling of a GPI anchored protein

In order to evaluate if the observed changes in the bilayer organization could affect a membrane protein distribution, SMase was applied to a supported lipid bilayer composed of DOPC:BSM:Chol 2:2:1 containing the glycosylphosphatidylinositol (GPI) anchored protein placental alkaline phosphatase (PLAP). GPI anchored proteins perform their function by association with raft domains.[27] We therefore chose it as a representative protein to study raft-associated proteins. Our preparation of PLAP partitions preferentially to the liquid ordered phase[28], (Fig. 2a). As Fig. 2 shows, the changes observed in lipid organization upon SMase incubation were simultaneously observed in the protein organization. The sequence in time is: domain coexistence–homogeneous bilayer–domain coexistence. PLAP partitions preferentially into the ceramide-enriched domains (dark regions) present at long incubation times over the brighter phase, and this preference seems stronger than in the initial case of liquid

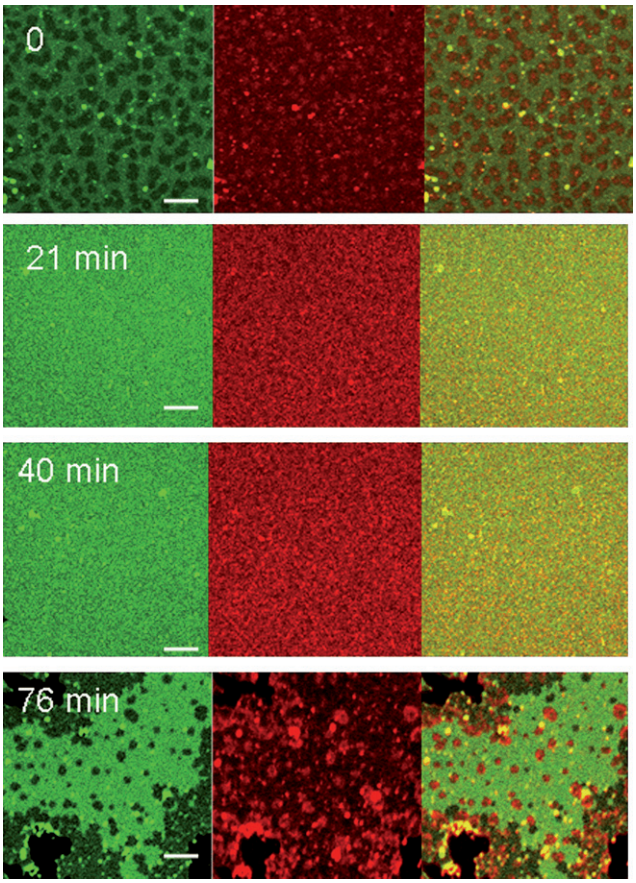

Fig. 2 Supported lipid bilayer containing GPI-anchored PLAP under the activity of sphingomyelinase. The numbers indicate the time with respect to addition of enzyme. The initial membrane composition is DOPC:BSM:Chol: 2:2:1. The protein:lipid ratio is 1:4000. In green, BODIPYChol, in red, rhodamine-labeled PlAP. The bars indicate 5 μm.

ordered–liquid disordered phase coexistence. This observation is in agreement with our previous observation of strong enrichment of PLAP in C18Cer domains.[28]

Reproducing the effect of SMase in pre-mixed membranes

In order to be able to evaluate the physical properties of the coexisting domains at different ceramide contents, we prepared bilayers with different amounts of BCer by pre mixing the lipids. BCer concentration increased at the expense of BSM. Imaging of supported bilayers shows, at concentrations of BCer between 10 and 20 mole%, the coexistence of three phases (Fig. 3, upper row). Apart from a dark and a bright phase, a third phase of intermediate brightness is observed. At higher BCer content (25–30 mole%), only two phases are observed, again one dark and one bright.

Further insight into the nature of the coexisting domains is gained by imaging of GUVs prepared with these mixtures, since the free standing bilayers are able to relax the line tension between domains much faster than the supported bilayers. GUVs made of the DOPC:BSM:Chol 2:2:1 mixture show big, circular domains (Fig. 3, lower row). The fluorescent probe used (BODIPYChol) partitions more strongly into the liquid disordered than into the liquid ordered phase. In coincidence with what is observed in the supported bilayers, the mixtures with 10–20 mole% BCer show the coexistence of three phases: one bright, one dark, and one of intermediate brightness. At 10 mole% BCer the domains are circular and big. The addition of 15 mole% BCer produces a dramatic change in the geometry of the domains. The intermediate and the dark domains become very small (in the resolution limit at approx 300 nm) and arrange in branched structures that percolate the GUV surface while the bright phase occupies the rest of the surface area between the branches. The highly branched geometry of these domains could indicate a lowered line tension that allows for the maintenance of a high amount of boundary lipid. In contrast, at lower amounts of ceramides and in its absence the domains are always round, indicating a high line tension that provides the driving force to maintain the circular shape of the domains.

At 20 mole% BCer, the GUVs show three phases also, but the GUV population is heterogeneous (see ESI,‡ Fig. S1). The geometry of the domains still seems to indicate a low line tension between the coexisting phases, since highly branched structures, very small circular domains and very elongated domains can be observed. In some GUVs however, only two phases are observed and the darker domains show straight borders that could indicate the presence of a gel phase. The domains geometry does not change after 2–4 h at room temperature.

Higher BCer concentrations (25–30 mole%) give rise to more ordered domains. These domains seem to be very rigid because the surface of the GUV is not a smooth sphere but becomes deformed, following the shape of the domains. At 30 mole% BCer, the domains look like crystals, with polygonal shapes and sharp edges (Fig. 3, lower row). This is likely due to the presence of a gel phase characterized by long range (macroscopic) order.

Physical characterization of the mixtures

In order to evaluate in a quantitative way the physical state of the coexisting domains, we performed fluorescence correlation spectroscopy (FCS) on the supported bilayers. FCS provides information on the diffusion coefficient of the lipids in the bilayer by analyzing the fluctuations in time of the fluorescence intensity of a probe that has been incorporated in the lipid mixture. The results obtained for our mixtures are shown in Table 1.

As observed by fluorescence imaging, the presence of 10 mole% of BCer induces the coexistence of three kinds of domains. These have different diffusion coefficients that can be identified with the liquid ordered phase, the liquid disordered phase and a third intermediate phase. The fact that the FCS curves can be successfully fit with a one component model excludes the possibility of the intermediate phase arising from an asymmetric distribution of lipids in the two hemilayers of the supported bilayer. The increase in BCer concentration to 15 mole% also induces the presence of three phases in supported bilayers, a bright phase, an intermediate phase, and a variable amount of dark phase. The diffusion coefficient of the bright phase diminishes with increasing BCer concentration, while the diffusion coefficient in both the intermediate phase and the dark phase increases with increasing BCer concentration. At 15 mole% BCer, the three coexisting phases show very similar diffusion coefficients. The FCS data indicate that the highly branched structures and very small circular domains observed in

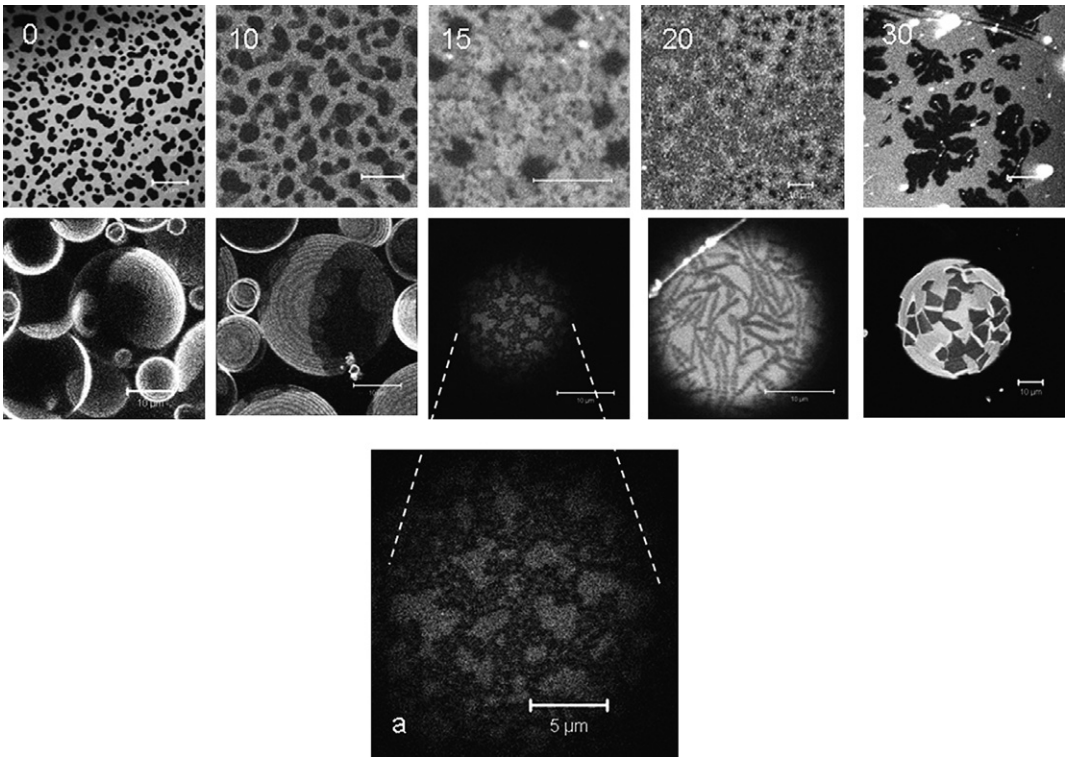

Fig. 3 Confocal fluorescence images of model membranes prepared by premixing of lipids. The upper row shows supported bilayers, the lower row shows GUVs. The numbers indicate the amount of BCer in mole% in the mixtures. The picture labeled (a) is a zoom-in of the 15 mole% GUV. The composition was DOPC:BSM:BCer:Chol 2:(2−X):X:1. The fluorescent probe used is BODIPYChol. The bars indicate 10 μm in all images except (a) where the bar shows 5 μm.

Table 1 FCS data on supported bilayers containing varying amounts of BCer. The results are the mean of at least 10 measurements. The temperature of the sample was 26 ± 1 °C. The fluorescent probe used was BODIPYChol

	Diffusion coefficient/μm^2 s^{-1}		
Composition DOPC:BSM:BCer:Chol (mole% of BCer)	Bright phase	Intermediate phase	Dark phase
2:2:0:1 (0%)	6.2 ± 0.4		0.3 ± 0.4
2:1.5:0.5:1 (10%)	5.2 ± 0.6	0.7 ± 0.3	0.1 ± 0.3
2:1.25:0.75:1 (15%)	3.0 ± 0.4	1.9 ± 0.3	1.1 ± 0.3
2:1:1:1 (20%)	2.4 ± 0.4	2.0 ± 0.4	< 0.01
2:0.75:1.25:1 (25%)	2.1 ± 0.5	—	< 0.01

the 15 mole% samples are probably maintained due to low line tension and not due to high viscosity, since the diffusion coefficient measured indicates fluid phase coexistence. At 20 mole%, the bright phase again shows a smaller diffusion coefficient than at 15 mole%. The intermediate phase does not change. The darker phase seems to have a high viscosity (like a gel phase) since the fluorescence becomes very rapidly bleached, not allowing for FCS measurement. At 25 mole%, only two phases are observed. The bright phase has an even smaller diffusion coefficient than at 20 mole%, although it can still be considered as a fluid phase. The darkest phase is again probably a gel phase.

Since the mixture containing 15 mole% of BCer seems to be the most similar to the homogeneous bilayer observed at intermediate times in supported bilayers under the activity of SMase, we decided to characterize it further with simultaneous AFM and confocal imaging. We used three different dyes to study this mixture: BODIPY-FChol, BODIPYChol and DiDC18. Fig. 4 shows that the three coexisting phases have height differences of: low-to-intermediate phase, 0.4 nm; intermediate-to-high phase, 0.2 nm. The simultaneous imaging with AFM and fluorescence allows the identification of the different phases. We show in Fig. 4 the comparison between the AFM imaging and the fluorescence imaging with DiDC18 and BODIPYChol. According to BODIPYChol fluorescence intensity, the bright phase is the lowest, the intermediate phase has intermediate height and the darkest phase is the highest. If we complement this information with the FCS data, we can say that this probe partitions more easily into the most disordered phases and becomes increasingly excluded from the increasingly ordered phases. Interestingly, DiDC18 partitions in a different way: it displays highest intensity in the lowest domains, intermediate intensity in the highest domains and lowest intensity in the domains with intermediate height (Fig. 4b). According to BODIPY-FChol fluorescence intensity (not shown), the bright phase is the one with intermediate height, the phase with intermediate brightness is the shortest, and the darkest phase is the tallest. Considering this last probe as the best to follow the behavior of unlabeled cholesterol,[29] we could say that the highest phase is depleted of cholesterol (probably because of a high enrichment in ceramides), the phase with intermediate height is the one most enriched in cholesterol, and the lowest phase has an intermediate amount of cholesterol.

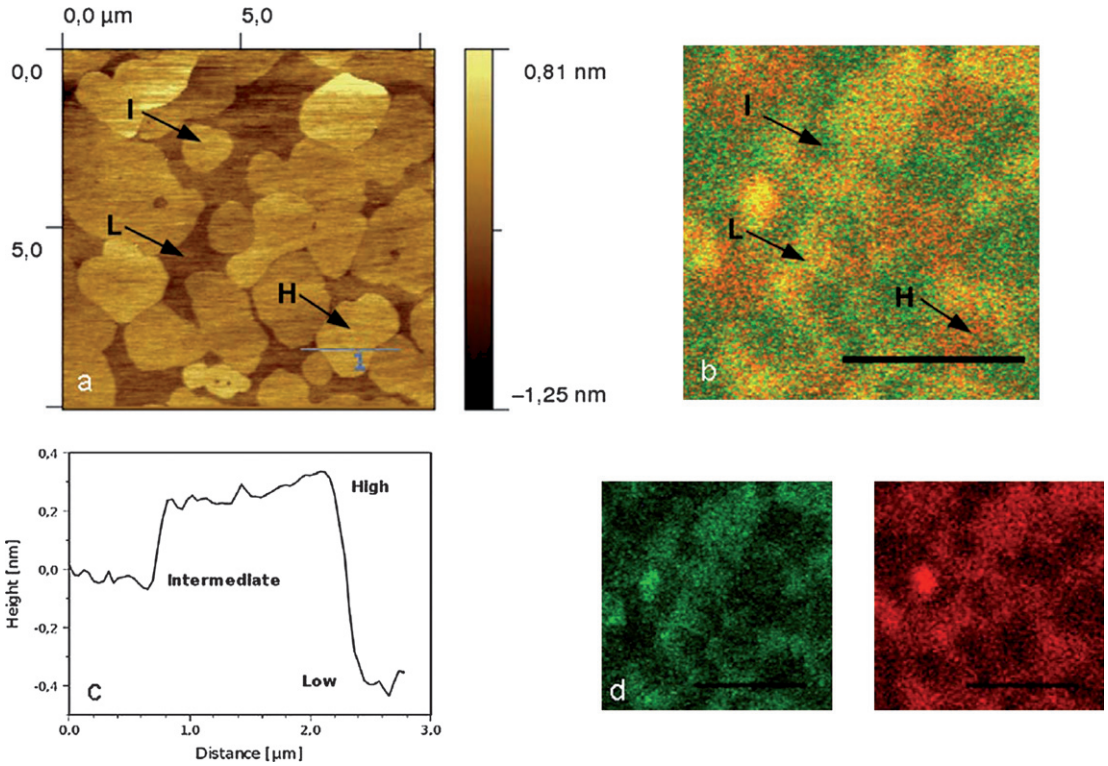

Fig. 4 Confocal fluorescence imaging and AFM imaging of the sample containing 15 mole% BCer. The coexisting domains are labeled high (H), intermediate (I) and low (L). (a) AFM image, (b) confocal fluorescence image, (c) height profile along the line in (a), (d) separate images of the two channels in the region shown in (b). BODIPYChol is shown in green and DiD in red. The bars indicate 5 µm.

In order to gain information on the thermodynamic characteristics of our samples, we performed differential scanning calorimetry (DSC) on mixtures containing different amounts of BCer (Fig. 5). The mixture of DOPC:BSM:Chol 2:2:1 shows a broad transition ending at 42 °C. The incorporation of 10 mole% BCer sharpens the transition slightly and shifts it to higher temperature (T_m is 41.3 °C). At 15 mole% BCer the transition has only slightly shifted upwards, with a T_m of 44.4 °C. At 20 mole% of BCer the main peak remains at the same position with a T_m of 44.4 °C but it shows a high temperature shoulder at approx. 49 °C. This may indicate the onset of the formation of a gel phase. When all of the BSM is replaced by BCer, three endothermic peaks appear, with T_ms of 26.1, 47.4 and 78.4 °C respectively.

Symmetric-homogeneous *vs* asymmetric-heterogeneous ceramides

In order to compare the organization of domains enriched in ceramides with different chains, we imaged GUVs composed of DOPC:C18SM:C18Cer:Chol 2:1.4:0.6:1 (12 mole% C18Cer) by confocal microscopy using two different fluorescent probes: DiDC18 and BODIPY-FChol. We have shown before that BODIPY-FChol partitions strongly into both liquid disordered and liquid ordered phases but is excluded from ceramide-enriched gel phases.[28] Fig. 6 shows that the GUVs containing C18Cer show three phases: a liquid disordered phase (where both BODIPY-FChol and DiD partition strongly), a liquid ordered phase (DiD partitions poorly but BODIPY-FChol partitions strongly) and a gel phase (where both probes are excluded). Previous work done in our lab has shown that C18Cer induces the formation of a gel phase at concentrations above 4 mole%.[9] Also the activity of SMase on supported bilayers composed of DOPC:C18SM:Chol produces from the beginning a gel phase enriched in C18Cer.[9]

We performed DSC on samples containing C18Cer in order to compare it with BCer. The results are shown in Fig. 5. The mixture of DOPC:C18SM:Chol 2:2:1 shows a broad phase transition that starts around 14 °C and ends at 55 °C. The incorporation of 10 mole% C18Cer sharpens the transition strongly so that now a T_m can be measured at 43.3 °C. The change in the shape of the calorimetric curve is also reflected in an increase of the cooperative unit[8] of the transition. This main peak shows a smaller second peak as a high temperature shoulder at 47.7 °C. At 15 mole% C18Cer the main peak slightly shifts to lower temperature, with a T_m of 42.3 °C, and the high temperature shoulder is more evident at 49.9 °C. At 20 mole% of C18Cer, two peaks appear, with T_m of 40.9 and 83.9 °C respectively. This last peak shows smaller peaks in the low temperature side, approx. at 72.4 and 76.5 °C. When all of the C18SM is replaced by C18Cer, two transitions, with T_m values of 42.5 and 78.5 °C, are evident. Both peaks show shoulders on the low temperature side. We interpret the shoulder in the 10 mole% sample as the melting of a ceramide enriched gel phase. This interpretation is supported by the fact that this shoulder increases in importance and is displaced to higher temperatures as the C18Cer concentration increases. At 20 mole% C18Ceramide, the amount of ceramide is high enough to allow for the formation of a gel phase composed purely of ceramides, as indicated by the presence of a peak at 83.9 °C.

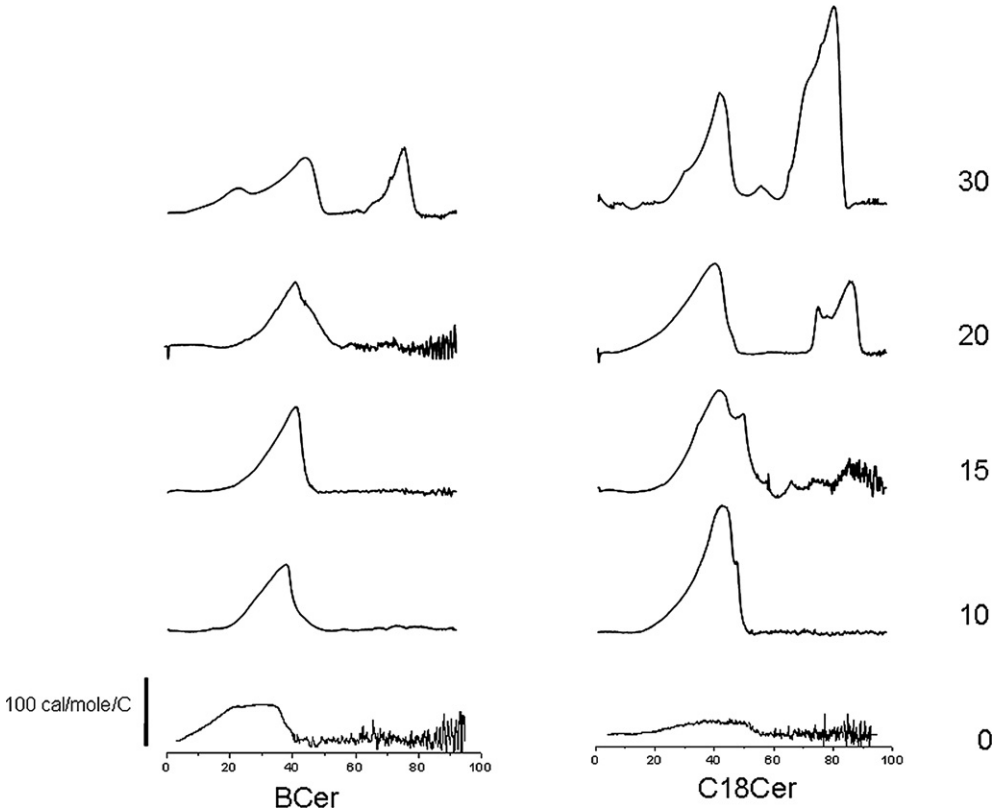

Fig. 5 Calorimetry of lipid mixtures containing BCer *versus* C18Cer. The composition of the mixtures was DOPC:SM:Cer:Chol 2:(2-X):X:1. The numbers on the right indicate the amount of ceramides in mole%.

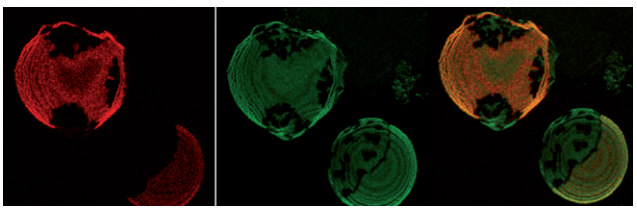

Fig. 6 Confocal fluorescence images of GUVs containing C18Cer. The composition of the membrane was DOPC:SM:Cer:Chol 2:1.4:0.6:1. In red, DiDC18, in green, BODIPY-FChol.

The comparison of the curves for BCer and C18Cer in Fig. 5 shows a similar pattern of effects induced by both ceramides: a sharpening of the transition peak with respect to mixtures without ceramides with a concomitant increase of the cooperative unit, the appearance of high temperature shoulders, and finally the appearance of a high temperature peak that most probably corresponds to the melting of a pure ceramide phase.[30] The difference between ceramides is the concentration necessary to induce these changes. While BCer induces a high temperature shoulder at 20 mole% and an all-ceramide peak at 30 mole%, C18Cer already induces a high temperature shoulder at 10 mole% and an all-ceramide peak at 20 mole%. Furthermore, since we already observe gel phase domains in GUVs containing 12 mole% C18Cer, it is possible to interpret the high temperature shoulders induced by C18Cer at 10 and 15mole% as all-ceramide domains melting. The fact that they melt not at 80 °C but at lower temperatures could be explained by the small amount of phase present and the fact that the domains are dispersed, which would result in looser packing and thus for a lower phase transition temperature. The same reasoning can be applied to the high temperature shoulder in the 20 mole% BCer mixture. In summary, while BCer can induce a gel-like, all-ceramide phase at concentrations of 20 mole% and higher, C18Cer is able to induce the formation of such domains at 10–12 mole%.

Conclusions

Bilayers composed of DOPC:BSM:Chol and containing a GPI-linked, membrane associated protein show the following changes under the effect of SMase: domain separation–homogeneous distribution–domain separation. This pattern of change is in contrast to what has been observed when applying SMase to mixtures containing homogenous symmetric SM, such as C18SM or egg SM. In these last cases, SMase has been shown to induce ceramide-enriched, gel phases that exclude fluorescently labeled lipids and show heights higher than liquid ordered domains.[9,31] No such effect as the homogeneization of the bilayer has been shown with symmetric SM. This effect is particularly interesting since it could produce an uncommon reshuffling of membrane components if it were to happen in a cellular membrane.

Since we wanted to know at which BCer concentration these changes were taking place, we decided to attempt to reproduce the effect of SMase by pre-mixing the lipids. We could not find

a composition at which the membrane in equilibrium showed complete homogeneity (data not shown). This is probably due to a non-equilibrium distribution of the lipids when under the activity of the enzyme.[32]Our results show that the membrane composition most similar to the homogeneous membrane we observe with SMase is probably around 15 mole% BCer. At this composition, the coexisting domains look similar with respect to the partitioning of the fluorescent probes, the diffusion coefficient measured by FCS, and the fact that the line tension seems to be strikingly reduced between the domains. On the other hand, confocal microscopy of GUVs containing a similar concentration of C18Cer shows clearly the presence of gel phase domains, in coexistence with liquid ordered and liquid disordered phases. We have shown previously that these domains strongly immobilize and sequester the GPI membrane-anchored protein, PLAP.[28]

Further information as to the differences in the membrane organization induced by homogeneous symmetric ceramides and brain ceramides is given by calorimetry. This technique shows that, while C18Cer can induce a gel phase at only 10 mole%, BCer needs to be present at 20 mole% in order to produce a similar effect. Calorimetry also shows that at high enough concentrations, both ceramides form a phase that is most likely pure ceramide, since the melting temperature is very high (78–84 °C).

The fact that the presence of ceramide molecules with asymmetric and heterogeneous chains produces a homogeneization of the membrane and a reshuffling of both lipids and lipid-linked proteins at concentrations of ~15%, while symmetric homogeneous ceramides produce gel phases that immobilize proteins at these concentration is of interest for membrane biology since this range of ceramide concentrations is thought to be representative of the amounts of ceramide present in signaling events in cells.[6,7] Indeed, a recent article has shown that the chain composition of ceramide can have profound effects in the outcome of the signaling events produced by this molecule: in cancerous cells, the presence of C24 and C24:1Cer has been shown to aid survival while C18Cer produced apoptosis.[17] We speculate that these different outcomes could be related to differences in membrane organization, with the asymmetric long ceramides producing reshuffling and bringing together molecules that were previously compartmentalized in rafts, while the symmetric ceramides produce further strong compartmentalization and isolation of membrane components.

The induction of increased order in previously disordered phases and of increased fluidity in previously viscous phases, thus giving rise to a new phase of intermediate fluidity, is the typical effect of cholesterol. Thus the results obtained with FCS on the 15 mole% BCer mixture give full support to our previous hypothesis.[24] Asymmetric heterogenous ceramides seem to have, at least in some range of concentrations, effects very similar to those of cholesterol.

Experimental

Chemicals

1,2-Dioleoyl-*sn*-glycero-3-phosphocholine (dioleoyl-phosphatidylcholine; DOPC), N-stearoyl-D-erythro-sphingosylphosphorylcholine (stearoyl sphingomyelin; C18SM), brain sphingomyelin (BSM), N-stearoyl-D-erythro-sphingosine (C18:0 ceramide, C18Cer), brain ceramides (BCer), and cholesterol were purchased from Avanti Polar Lipids (Alabaster, AL) and used without further purification. BODIPY free cholesterol analogue 23-(4,4-difluoro-1,3,5,7-tetramethyl-4-bora-3a,4a-diaza-*s*-indacen-8-yl)-24-norchol-5-en-3β-ol (BODIPY-FChol) was provided by Dr Robert Bittman. Dioctadecyl-3,3,3′,3′-tetramethylindodicarbocyanine perchlorate (DiDC18), cholesteryl 4,4-difluoro-5,7-dimethyl-4-bora-3a, 4a-diaza-*s*-indacene-3-dodecanoate (cholesteryl ester BODIPY FL C_{12}, BODIPYChol), were from Invitrogen (Eugene, OR). Optical Adhesive 88, used to glue the mica on coverslips, was purchased from Norland Products (Cranbury, NJ). Alkaline phosphatase from human placental tissue (PLAP), 3-[(3-cholamidopropyl) dimethylammonio]-1-propanesulfonic acid (CHAPS) and sodium cholate were purchased from Sigma. Before use, PLAP was purified and labelled with NHS-rhodamine (Pierce, Rockford, IL) as described in ref. 23.

Supported lipid bilayers (SLBs)

Planar bilayers were prepared based on the procedure described in Chiantia *et al.*[9] Briefly, lipids and fluorescent lipid analogues were mixed in organic solvents in different proportions. The concentration of fluorescent lipid analogues was always 0.1 or 0.01 mol%, for imaging and FCS respectively. After solvent evaporation, the lipid film thus obtained was rehydrated using buffer at 2 mg/mL lipid concentration and resuspended by vigorous vortexing and heating above the phase transition temperature. After sonication of the suspension at 60 °C, a small aliquot was deposited on a ~10 μm thick, freshly cleaved mica, glued to a glass coverslip. The coverslip was sealed in the temperature-controlled Biocell stage (JPK Instruments, Berlin, Germany) for AFM imaging or in a hand made cell for FCS. The sample was rinsed at the same temperature at least 10 times with buffer and then allowed to cool down first to 40 °C and then to room temperature. The buffer contained 150 mM NaCl, 10 mM Hepes, 3 mM NaN_3, pH 7.4 and was filtered through 0.2 μm pore membranes before use.

Protein-containing SLBs

In the case of membranes containing rhodamine-labeled Placental Alcaline Phosphatase (PLAP), the liposomes were used to produce proteoliposomes before deposition onto mica as described in ref. 23. Briefly, the protein and liposomes were mixed to final concentrations of 40 μg/mL and 2.5 mg/mL respectively, in the presence of 1.8% CHAPS. The initial protein:lipid ratio was ~1:2500. After 24 h dialysis against buffer A using a 50 kDa SpectraPro membrane (Spectrum, Breda, Netherlands), a small aliquot was diluted 10 times, briefly sonicated with liposomes in the desired proportions at 50 °C, and deposited onto mica as described above for the protein-free, liposomes. The final protein:lipid ratio was then ~1:4000. The activity of the reconstituted protein was checked by enzymatic digestion of Sigma Fast p-nitrophenyl phosphate (Sigma) in the solution above the SLB.

Giant unilamellar vesicles

GUVs were prepared by electroformation[28] on custom made Teflon and Pt wire chambers.[29,30] Lipid mixtures in chloroform:methanol 2:1 (10 mg/ml) were deposited as small droplets on the preheated Pt wires and the solvent was evaporated at 50 °C for 5 min. After adding a 200 mOsM sucrose solution to the chamber, a voltage of 2.3 V at 10 Hz was applied for 2 h at 65–67 °C. An aliquot (100 μl) of the GUVs thus formed were transferred to a LabTech chamber containing 400 μl of a 200 mOsM glucose solution.

Optical setup

Confocal imaging and FCS measurements were performed on an laser scanning microscope (LSM) Meta 510 system (Carl Zeiss, Jena, Germany) using a 40X NA 1.2 UV-VIS-IR C Apochromat water-immersion objective and a home-built detection unit at the fiber output channel. An appropriate band-pass filter was used behind a collimating achromat to reject the residual laser and background light. Another achromat (LINOS Photonics, Goettingen, Germany) with a shorter focal length was used to image the internal pinhole onto the aperture of the fiber connected to the avalanche photo diode (APD, PerkinElmer, Boston, MA). The photon arrival times were recorded in the photon mode of the hardware correlator Flex 02-01D (Correlator.com, Bridgewater, NJ). All filters and dichroic mirrors were purchased from AHF Analyse Technik, Tuebingen, Germany. The movement of the detection volume was controlled directly with the Zeiss LSM operation software. Imaging and FCS measurements were performed at room temperature. For FCS measurements, we used the z-scan method to evaluate the radius of the detection area on the plane of the membrane. For details on the FCS z-scan method see ref. 21.

Atomic force microscopy

AFM measurements were performed using a NanoWizard system (JPK Instruments, Berlin, Germany) mounted on the LSM Meta 510 system described in the optical setup paragraph. Contact-mode topographic images were taken in the constant-deflection mode using uncoated silicon cantilevers (MikroMasch, Spain) with a typical spring constant of 0.03 Nm^{-1}. The force applied on the sample was maintained at the lowest possible value by continuously adjusting the set point during imaging. The scan rate was set to 1–2 Hz. The height and deflection signals were collected simultaneously in both trace and retrace directions. Images were line-fitted as required. Isolated scan lines were occasionally removed. Imaging was performed at room temperature.

Calorimetry

Aqueous lipid dispersions were prepared by premixing the lipids in the desired proportions from solutions in chloroform:methanol 2:1. The mixture was taken to dryness as a thin film in a glass tube under N_2 and submitted to vacuum for 2–4 h. Multilamellar vesicles were obtained by hydrating the lipid with MilliQ water (18 MΩ) and subsequent vortexing and heating to 85 °C. After degassing, the sample was introduced into the sample cell of a high sensitivity differential scanning calorimeter (MicroCal, GE Healthcare Europe, Munich, Germany). The reference cell was filled with MilliQ water. The lipid concentration was 7 mM. Samples were run at 45 °C/h in duplicate.

References

1 M. Nikolova-Karakashian, A. Karakashian and K. Rutkute, *Subcell. Biochem.*, 2008, **49**, 469–86.
2 H. Grassme, V. Jendrossek, A. Riehle, G. von Kurthy, J. Berger, H. Schwarz, M. Weller, R. Kolesnick and E. Gulbins, *Nature Medicine*, 2003, **9**, 322–330.
3 H. Grassme, A. Riehle, B. Wilker and E. Gulbins, *J. Biol. Chem.*, 2005, **280**, 26256–262.
4 B. Ogretmen and Y. Z. Hannun, *Nat. Rev. Cancer*, 2004, **4**, 604–616.
5 C. R. Bollinger, V. Teichgraber and E. Gulbins, *Biochim. Biophys. Acta*, 2005, **1746**, 284–94.
6 A. E. Cremesti, F. M. Goñi and R. Kolesnick, *FEBS Letters*, 2002, **531**, 47–53.
7 Y. A. Hannun, *Science*, 1996, **274**, 1855–1859.
8 D. C. Carrer and B. Maggio, *J. Lipid Res.*, 1999, **40**, 1978–1989.
9 S. Chiantia, N. Kahya, J. Ries and P. Schwille, *Biophys. J.*, 2006, **90**, 4500–508.
10 H. W. Huang, E. M. Goldberg and R. Zidovetzki, *Biochem. Biophys. Res. Commun.*, 1996, **220**, 834–8.
11 J. Sot, F. J. Aranda, M. I. Collado, F. M. Goñi and A. Alonso, *Biophys. J.*, 2005, **88**, 3368–80.
12 F. X. Contreras, G. Basañez, A. Alonso, A. Herrman and F. M. Goñi, *Biophys. J.*, 2005, **88**, 348–59.
13 J. M. Holopainen, M. I. Angelova and P. K. Kinnunen, *Biophys. J.*, 2000, **78**, 830–38.
14 K. Trajkovik, C. Hsu, S. Chiantia, L. Rajendran, D. Wenzel, F. Wieland, P. Schwille, B. Brugger and M. Simons, *Science*, 2008, **319**, 1244–47.
15 A. Morales, H. Lee, F. M. Goñi, R. Kolesnick and J. C. Fernandez-Checa, *Apoptosis*, 2007, **12**, 923–39.
16 F. M. Goñi and A. Alonso, *Biochim. Biophys. Acta*, 2006, **1758**, 1902–21.
17 A. F. Saad, W. D. Meacham, A. Bai, V. Anelli, S. Elojeimy, A. E. Mahdy, L. S. Turner, J. Cheng, A. Bielawska, J. Bielawski, T. E. Keane, L. M. Obeid, Y. A. Hannun, J. S. Norris and X. Liu, *Cancer Biol. Ther.*, 2007, **6**, 1455–60.
18 J. M. Holopainen, H. L. Brockman, R. E. Brown and P. K. Kinnunen, *Biophys. J.*, 2001, **80**, 765–75.
19 Ira and L. J. Johnston, *Langmuir*, 2006, **22**, 11284–289.
20 Megha, P. Sawatzki, T. Kolter, R. Bittman and E. London, *Biochim. Biophys. Acta*, 2007, **1768**, 2205–212.
21 J. Sot, M. Ibarguren, J. V. Busto, L. R. Montes, F. M. Goñi and A. Alonso, *FEBS Letters*, 2008, **582**, 3230–236.
22 J. M. Holopainen, J. Lemmich, F. Richter, O. G. Mouritsen, G. Rapp and P. K. Kinnunen, *Biophys. J.*, 2000, **78**, 2459–69.
23 S. N. Pinto, L. C. Silva, R. F. M. de Almeida and M. Prieto, *Biophys. J.*, 2008, **95**, 2867–79.
24 D. C. Carrer, S. Schreier, M. Patrito and B. Maggio, *Biophys. J.*, 2006, **90**, 2394–403.
25 H. W. Huang, E. M. Goldberg and R. Zidovetzki, *Eur. Biophys. J.*, 1998, **27**, 361–66.
26 S. Chiantia, N. Kahya and P. Schwille, *Langmuir*, 2007, **93**, 103–112.
27 D. A. Brown and J. K. Rose, *Cell*, 1992, **68**, 533–544.
28 S. Chiantia, J. Ries, G. Chwastek, D. C. Carrer, Z. Li, R. Bittman and P. Schwille, *Biochim. Biophys. Acta*, 2008, **1778**, 1356–64.
29 M. Hölttä-Vuori, R. L. Uronen, J. Repakova, E. Salonen, I. Vattulainen, P. Panula, Z. Li, R. Bittman and E. Ikonen, *Traffic*, 2008, **9**, 1839–49.
30 J. Shah, J. M. Atienza, A. V. Rawlings and G. G. Shipley, *J. Lipid Res.*, 1995, **36**, 1945–55.
31 Ira and L. J. Johnston, *Biochim. Biophys. Acta*, 2008, **1778**, 185–97.
32 M. L. Fanani, L. De Tullio, S. Härtel, J. Jara and B. Maggio, *Biophys. J.*, 2009, **96**, 67–76.
33 M. I. Angelova and D. S. Dimitrov, *Faraday Discuss. Chem. Soc.*, 1986, **81**, 303–308.
34 A. J. García-Sáez, D. C. Carrer, P. Schwille in *Methods in Molecular Biology: Liposomes*, ed. V. Weissig, Humana Press, Totowa, New Jersey, in press.
35 M. Fidorra, L. Duelund, C. Leidy, A. C. Simonsen and L. A. Bagatolli, *Biophys. J.*, 2006, **90**, 4437–4451.

